Syntheses, Structures, and Reductive Elimination Studies of Six-Membered Diaryl Platinacycle Complexes

ARTICLE *in* ORGANOMETALLICS · FEBRUARY 2010

Impact Factor: 4.13 · DOI: 10.1021/om901033z

2 AUTHORS, INCLUDING:

Robert Robinson Jr
University of Tasmania
8 PUBLICATIONS **26** CITATIONS

1388 *Organometallics* **2010,** *29,* 1388–1395
DOI: 10.1021/om901033z

ORGANOMETALLICS
Article

Syntheses, Structures, and Reductive Elimination Studies of Six-Membered Diaryl Platinacycle Complexes

Robert Robinson Jr. and Paul R. Sharp*

125 Chemistry, University of Missouri—Columbia, Columbia, Missouri 65211

Received November 30, 2009

The six-membered platinacycles $PtL_2(C_6H_4XC_6H_4)$ (X = CH_2, O, NMe; L = PEt_3, L_2 = 1,3-bis(diphenylphosphino)propane (dppp), 4,4′-bis-*tert*-butyl-2,2′-bipyridine ($^tBu_2bpy$)), have been prepared from *cis*-PtL_2Cl_2 and the appropriate dilithio reagents. Reductive elimination studies on the platinacycles with L = PEt_3 show that the bridging group (X) dramatically influences the reductive elimination rate. Thermodynamic activation parameters were determined for the platinacycles and showed a $\Delta H^{\ddagger}$ trend X = NMe ≪ O < CH_2 with an essentially zero value for $\Delta S^{\ddagger}$. Rate constants at 95 °C show over a million-fold increase on going from X = CH_2 to X = NMe. DFT calculations support direct elimination without phosphine ligand loss and indicate a progressively earlier transition state in the series X = CH_2, O, NMe. The earlier transition state and the accelerated rate are associated with the beginning of aromatization in the eliminating organic unit. Computed thermodynamic activation parameters are in good agreement with the experimental results.

Introduction

Reductive elimination is an important and vital reaction in chemistry and is often the crucial step for product formation in metal-catalyzed organic synthesis reactions.[1] Both palladium(0) and nickel(0) complexes are commonly used as catalysts because of their high activity.[2,3] High activity implies short-lived intermediates, making isolation and study of intermediates very difficult. Analogous platinum(0) complexes are usually more stable and amenable to study. Diaryl Pt complexes of the formula *cis*-$PtL_2(C_6H_4R)(C_6H_4R')$ (L_2 = phosphines) can be isolated and undergo reductive elimination to give biaryls, $RC_6H_4-C_6H_4R'$ (eq 1), whereas the analogous Pd complexes cannot be isolated.[4] Reductive elimination studies of these Pt complexes have revealed interesting aryl substituent features. Increased reductive elimination rates are observed in symmetric complexes when the R groups are electron donating and even higher rates when one aryl group has an electron-withdrawing substituent and the other an electron-donating substituent.[5−7]

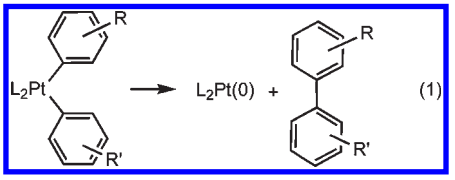

These studies are informative for simple diaryl complexes and the formation of biaryls. However, the formation of ring systems incorporating biaryls requires reductive elimination from metallacycle complexes.[8−12] Linking the aryl groups together in a metallacycle complex introduces additional factors in the reductive elimination process. Our group has shown that for Pt and Pd four- and five-membered metallacycles where the aryl groups have been linked into a polycyclic framework simple reductive elimination is shut down.[13,14] Instead, apparent bimolecular reductive elimination occurs catalytically on colloidal metal surfaces after transfer of the metallacycle ring from the complex to the metal colliod surface. In the presence of alkynes cycloaddition reactions also occur on the colloid surface. In this paper we report our work on reductive eliminations from six-membered platinacycles

*Corresponding author. E-mail: SharpP@missouri.edu.

(1) Crabtree, R. H. *The Organometallic Chemistry of the Transition Metals*, 4 ed.; Wiley: New York, 2005.
(2) Brandsma, L.; Vasilevsky, S. F.; Verkruijsse, H. D. *Application of Transition Metal Catalysts in Organic Synthesis*; Springer-Verlag: New York, 1999.
(3) Tsuji, J. *Palladium Reagents and Catalysts: New Perspectives for the 21st Century*, 2nd ed.; J. Wiley: Chichester, 2004.
(4) Braterman, P. S.; Cross, R. J.; Young, G. B. *J. Chem. Soc., Dalton Trans.* **1976**, 1306–1310.
(5) Brune, H. A.; Stapp, B.; Schmidtberg, G. *J. Organomet. Chem.* **1986**, *307*, 129–137.
(6) Brune, H. A.; Stapp, B.; Schmidtberg, G. *Chem. Ber.* **1986**, *119*, 1845–56.
(7) Shekhar, S.; Hartwig, J. F. *J. Am. Chem. Soc.* **2004**, *126*, 13016–13027.
(8) Ma, S.; Gu, Z. *Angew. Chem., Int. Ed.* **2005**, *44*, 7512–7517.
(9) Garcia-Cuadrado, D.; Braga, A. A. C.; Maseras, F.; Echavarren, A. M. *J. Am. Chem. Soc.* **2006**, *128*, 1066–1067.
(10) Campeau, L. C.; Parisien, M.; Jean, A.; Fagnou, K. *J. Am. Chem. Soc.* **2006**, *128*, 581–590.
(11) Campo, M. A.; Huang, Q.; Yao, T.; Tian, Q.; Larock, R. C. *J. Am. Chem. Soc.* **2003**, *125*, 11506–11507.
(12) Catellani, M.; Motti, E.; Faccini, F.; Ferraccioli, R. *Pure Appl. Chem.* **2005**, *77*, 1243–1248.
(13) Begum, R. A.; Chanda, N.; Ramakrishna, T. V. V.; Sharp, P. R. *J. Am. Chem. Soc.* **2005**, *127*, 13494–13495.
(14) Chanda, N.; Sharp, P. R. *Organometallics* **2007**, *26*, 1635–1642.

 Published on Web 02/23/2010

Table 1. Selected ^{195}Pt, ^{31}P, and ^{13}C NMR Data for 1−5[a]

	δ ^{195}Pt	δ ^{31}P (J_{Pt-P})	δ C1[d] ($^1J_{C-Pt}$, $^2J_{C-Ptrans}$)
1[b,c]	−4574	4.8 (1833)	161.5 (806.5, 116.7)
2[b]	−3112	5.0 (2014)	145.3 (769.7, 105.7)
3[e]	−4700	7.3 (1979)	not resolved
4[b]	−3079	3.6 (1902)	not resolved
5[b]	−3646		not resolved

[a] Chemical shifts (δ) in ppm and coupling constants (J) in Hz. [b] In $CDCl_3$. [c] Data from ref 15. [d] C1 = Pt-bonded carbon atom. [e] In THF at −40 °C.

where the aryl groups have been linked together by a bridging group in the *ortho* positions. We find that simple reductive elimination is turned back on and that, similar to the ring substituents in the diaryl complexes (eq 1), the bridging group influences the reductive elimination rate, but the effect is many orders of magnitude larger.

Results

Syntheses and NMR Spectra. Platinacycles **1**−**5** were synthesized by the reaction of *cis*-PtL_2Cl_2 (L = PEt_3, L_2 = dppp or ^{t}Bu$_2$bpy) with the appropriate dilithio reagents (eq 2). The synthesis of **1** by this method was previously reported.[15] With the exception of **3**, which could not be isolated due to its instability above −30 °C, the platinacycles were isolated in >80% yield. Complex **3** was characterized by NMR spectroscopy and by its decomposition products (see below). All other new platinacycles were fully characterized by NMR spectroscopy, X-ray crystallography, and elemental analysis. For comparison purposes, previously reported data for **1** are included below.

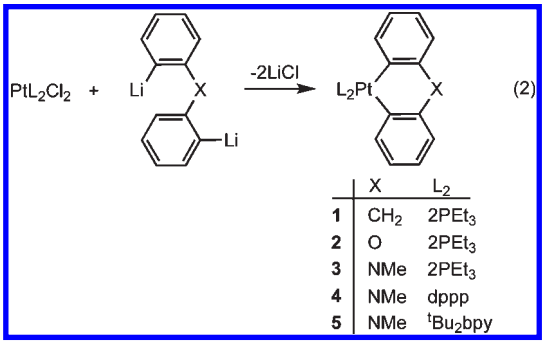

^{31}P and ^{195}Pt NMR spectroscopic data for the platinacycles are shown in Table 1. ^{31}P NMR spectra of **1**−**4** show singlets with ^{195}Pt satellites. Chemical shifts for the PEt_3 derivatives **1**−**3** lie in a narrow region (greatest difference ±3.2 ppm), consistent with nearly equivalent chemical environments for the ^{31}P nuclei. ^{31}P−^{195}Pt coupling constants are typical for a phosphine ligand *trans* to an aryl group in Pt(II) complexes.[16] For **1**−**3** a trend is detected where the coupling constant increases in the order X = CH_2 < NMe < O, indicative of a decrease in the *trans* influence of the aryl group with increasing electronegativity of the bridging group.[17,18] ^{195}Pt NMR spectra all show triplets from ^{31}P coupling with no discernible trend in the shifts.

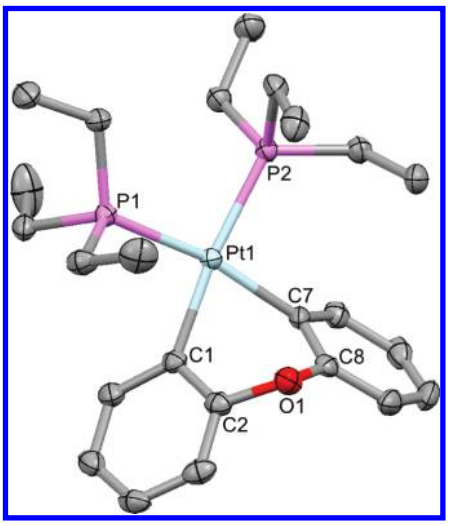

Figure 1. Molecular structure of $Pt(PEt_3)_2(C_6H_4OC_6H_4)$ (**2**) (50% probability ellipsoids, hydrogen atoms omitted for clarity).

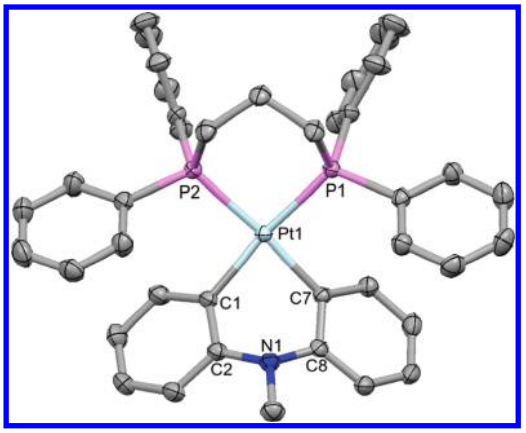

Figure 2. Molecular structure of $Pt(dppp)(C_6H_4NMeC_6H_4)$ (**4**) (50% probability ellipsoids, hydrogen atoms omitted for clarity).

All complexes exhibit the expected four aromatic proton and six aromatic carbon NMR signals for the two equivalent aryl rings. ^{13}C NMR data for the Pt-bonded carbon atoms (C1) of **1** and **2** are included in Table 1. Coupling constants are consistent with the *trans* influence trend in the ^{31}P−^{195}Pt coupling observed in the ^{195}Pt and ^{31}P NMR spectra. Both the ^{13}C−^{195}Pt and the ^{13}C−^{31}P coupling decrease from **1** to **2**, indicating a weaker donor on going from X = CH_2 to X = O.

X-ray Structures. The solid-state structures of **2**, **4**, and **5** are depicted in Figures 1−3, with selected metrical parameters listed in Table 2. These three complexes and **1**[15] differ only in the bridging group X and/or the ancillary ligand, and the overall structures are very similar. All of the complexes have slightly distorted square-planar environments surrounding the Pt center. In **2**, the L−Pt−L angle (P1−Pt1−P2) is 98.43(3)°, nearly identical to the previously reported value for **1** of 98.8(1)°. Smaller L−Pt−L angles are observed in **4** (90.58(3)°) and **5** (76.56(10)°). The N−Pt−N angle in **5** is controlled by the geometry of the bidentate ^{t}Bu$_2$bpy ligand. The smaller P−Pt−P angle in **4** is probably not enforced by the dppp ligand but rather may result from steric interactions between the PPh_2 groups and the platinacycle aryl rings. The C−Pt−C angle in **2** (80.31(11)°) is slightly smaller than

(15) Alcock, N. W.; Bryars, K. H.; Pringle, P. G. *J. Chem. Soc., Dalton Trans.* **1990**, 1433–1439.
(16) Dietrich, G.; Vimal, K. J.; Axel, K.; Thilo, S.; Stanislav, Z. L. *Eur. J. Inorg. Chem.* **2005**, *2005*, 4056–4063.
(17) Appleton, T. G.; Clark, H. C.; Manzer, L. E. *Coord. Chem. Rev.* **1973**, *10*, 335–422.
(18) Appleton, T. G.; Bennett, M. A. *Inorg. Chem.* **1978**, *17*, 738–47.

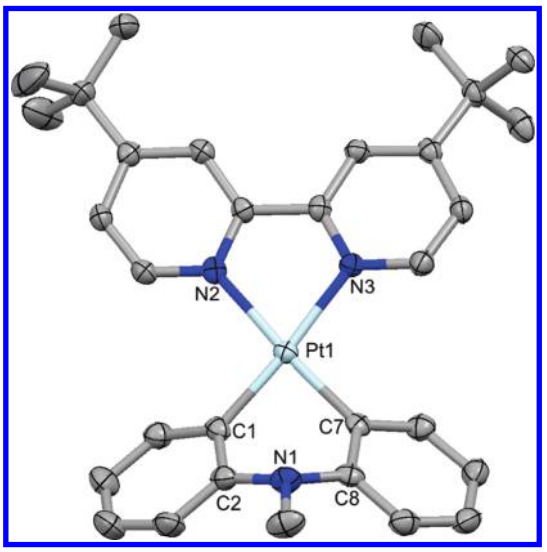

Figure 3. Molecular structure of Pt(^{t}Bu$_2$bpy)(C$_6$H$_4$NMeC$_6$H$_4$) (**5**) (50% probability ellipsoids, hydrogen atoms omitted for clarity).

Table 2. Selected Metrical Parameters (distances in Å and angles in deg) for Platinacycles 1, 3, 4, and 5[a]

	1 (X = CH$_2$)	**2** (X = O)	**4** (X = NMe)	**5** (X = NMe)
Pt−C	2.062(11)	2.062(3)	2.046(3)	1.993(3)
	2.038(11)	2.059(3)	2.058(3)	1.992(3)
	av = 2.050(17)	av = 2.060(2)	av = 2.052(8)	av = 1.992(1)
Pt−L	2.303(3)	2.321(1)	2.3072(7)	2.120(3)
	2.323(3)	2.330(1)	2.3144(7)	2.120(3)
	av = 2.313(14)	av = 2.326(6)	av = 2.311(5)	av = 2.120(0)
C2−X	1.531(17)	1.410(3)	1.418(4)	1.408(5)
	1.512(14)	1.411(4)	1.419(3)	1.420(4)
	av = 1.522(13)	av = 1.410(1)	av = 1.419(1)	av = 1.414(8)
C1---C7	2.67(2)	2.658(4)	2.697(3)	2.688(6)
C1−Pt−C7	81.3(4)	80.32(11)	82.17(10)	84.82(13)
L−Pt−L	98.8(1)	98.43(3)	90.58(3)	76.56(10)
C2−X−C8	107.5(9)	109.7(2)	116.6(2)	116.8(3)
fold angle[b]	69.5	66.6	58.0	51.4
ring angle[c]	74.7	69.4	53.8	48.6

[a] Numbers in parentheses indicate the estimated error in the last significant digit or for the averages (av) the standard deviation. [b] Acute angle between planes Pt1, C1, C2, X and Pt1, C7, C8, X. [c] Acute angle between C$_6$ ring planes C1−C6 and C7−C12.

that in **1** (81.3(4)°) but increases in **4** (82.17(10)°) and **5** (84.82(13)°). With both **2** and **4** containing phosphine ligands the average Pt−C (2.060(2) and 2.052(8) Å) and Pt−P (2.326(6) and 2.311(5) Å) bond distances are very similar and comparable to those in **1** (2.050(17) and 2.313(14) Å). Similarly, the average Pt−N and Pt−C bond lengths of 2.12 and 1.99 Å in **5** are typical of bpy phenyl complexes.[19−24]

As previously observed for **1**,[15] the Pt-containing six-membered ring of **2**, **4**, and **5** adopts a boat conformation with the Pt atom and the bridging group X at the "bow" and "stern". The fold angle, as defined by the acute angle between the two planes (Pt1, C1, C2, X and Pt1, C7, C8, X), decreases in the order **1** > **2** ≫ **4** > **5**. The two platinacycles **4** and **5** allow us to examine structural features associated with the NMe group that are not possible with unstable **3**. Both complexes show a substantially smaller angle than the X = O and CH$_2$ derivatives, **1** and **2**, indicating a greater tendency toward planarity for the X = NMe complexes. This is attributed to nitrogen lone pair donation into the aromatic rings of the platinacyclic system and is consistent with the near planarity of the N centers (sum of angles ~350°), the short average C−N distance (1.414 Å), and the small angle between the aryl ring planes (48.6°).

Table 3. Experimental (exptl)[a] and Computational (DFT)[b] Thermodynamic Data

	$\Delta H^{\ddagger}$ (kcal/mol)		$\Delta S^{\ddagger}$ (cal/K·mol)	
	exptl	DFT	exptl	DFT
1 or **1′** (X = CH$_2$)	29.0(9)	27.4	−4.2(3)	3.8
2 or **2′** (X = O)	25.9(6)	23.9[c]	−3.1(2)	0.8[c]
3 or **3′** (X = NMe)	21(2)	18.4	6(2)	4.3

[a] In toluene. [b] T = 298 K, gas phase, with PMe$_3$ in place of PEt$_3$. [c] Optimization not converged (see text).

Scheme 1

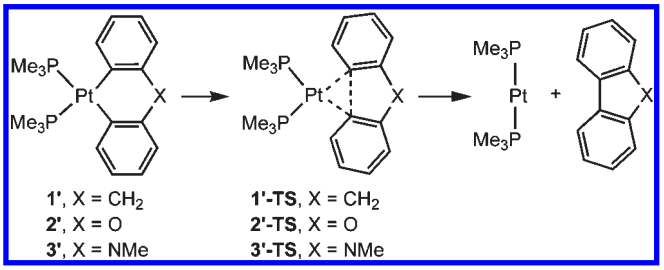

Reductive Elimination Studies. All three platinacycles **1**−**3** thermally decompose by reductive elimination with C−C bond formation (eq 3). This process occurs at comparable rates at −30 °C for **3**, 70 °C for **2**, and 110 °C for **1**. The products are fluorene (X = CH$_2$), dibenzofuran (X = O), and *N*-methylcarbazole (X = NMe) and the fragment Pt(PEt$_3$)$_2$. For subsequent kinetic studies PhCCPh was added to trap the Pt(PEt$_3$)$_2$ fragment, giving the stable and readily detected adduct Pt(PEt$_3$)$_2$(η^2-PhCCPh) (**6**). Control experiments indicated that PhCCPh, PEt$_3$, water, and O$_2$ additions to the reactions do not affect the reductive elimination rates. Reactions were followed by ^{31}P NMR spectroscopy over three half-lives, and plots of the concentration against time revealed first-order kinetics for all three platinacycles.

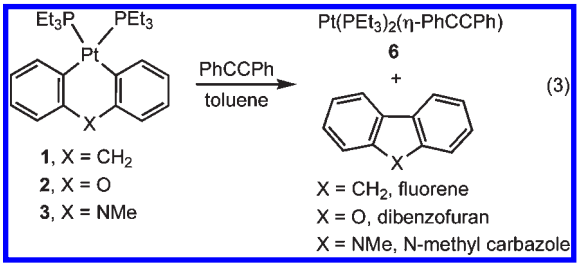

Rate constants for the reductive elimination reactions were determined at three different temperatures (Supporting Information). Extracted thermodynamic parameters are listed in Table 3. As expected from the reductive elimination

(19) De Crisci, A. G.; Lough, A. J.; Multani, K.; Fekl, U. *Organometallics* **2008**, *27*, 1765.
(20) Sun, Y.; Ross, N.; Zhao, S.-B.; Huszarik, K.; Jia, W.-L.; Wang, R.-Y.; Macartney, D.; Wang, S. *J. Am. Chem. Soc.* **2007**, *129*, 7510.
(21) Plutino, M. R.; Scolaro, L. M.; Albinati, A.; Romeo, R. *J. Am. Chem. Soc.* **2004**, *126*, 6470.
(22) Ong, C. M.; Jennings, M. C.; Puddephatt, R. J. *Can. J. Chem.* **2003**, *81*, 1196.
(23) Ng, Y.-Y.; Che, C.-M.; Peng, S.-M. *New J. Chem.* **1996**, *20*, 781.
(24) Klein, A.; Hausen, H.-D.; Kaim, W. *J. Organomet. Chem.* **1992**, *440*, 207.

Table 4. Selected Metrical Parameters (distances in Å and angles in deg) for DFT Optimized Structures[a]

	1′	**2′**	**3′**	**1′-TS**	**2′-TS**[b]	**3′-TS**
	(X = CH_2)	(X = O)	(X = NMe)	(X = CH_2)	(X = O)	(X = NMe)
Pt−C[b]	2.068	2.059	2.057	2.153	2.124	2.113
Pt−P[b]	2.420	2.420	2.419	2.372	2.381	2.382
X−C[b]	1.521	1.394	1.427	1.519	1.378	1.399
C1–C7	2.717	2.699	2.682	1.844	1.870	1.916
C1−Pt−C7	82.1	81.9	81.4	50.7	52.2	53.9
P−Pt−P	96.4	95.5	95.6	111.1	108.8	107.8
C2−X−C8	108.1	113.1	114.0	103.4	108.8	111.1
ring angle[c]	72.9	61.2	62.2	60.2	52.5	53.8

[a] Optimization not converged (see text). [b] Average distance. [c] Acute angle between C_6 ring planes C1−C6 and C7−C12.

temperatures, the $\Delta H^{\ddagger}$ values follow the trend **1** > **2** ≫ **3**, where the **2** and **3** gap is nearly twice that of **1** and **2**. The $\Delta S^{\ddagger}$ values are small, as expected for a unimolecular reaction. Overall, these activation parameters are quite comparable to those for biaryl elimination from $Pt((C_6F_5)_2PCH_2CH_2P(C_6F_5)_2)(Ph)_2$ in benzene ($\Delta H^{\ddagger}$ = 27.6 ± 1 kcal/mol, $\Delta S^{\ddagger}$ = −1.5 ± 1 cal/K·mol)[25] and fall into the range reported for elimination from a number of complexes of formula *cis*-$Pt(P(C_6H_4X)_3)_2(C_6H_4Y)(C_6H_4Z)$ ($\Delta H^{\ddagger}$ = 23.4 ± 0.4 to 34 ± 2 kcal/mol, $\Delta S^{\ddagger}$ = −5.9 ± 4.6 to 21 ± 7 cal/K·mol).[26]

Computational Studies. The platinacycle reductive elimination process was evaluated computationally in the gas phase using DFT. Model structures (**1′**, **2′**, and **3′**), where the PEt_3 ligand of **1**, **2**, and **3** was replaced with PMe_3, were optimized. A comparison of the calculated structures with the crystallographic structures showed reasonable agreement. A notable difference is the trend in fold angles: 66.17° for **1′**, 61.01° for **2′**, and 62.21° for **3′**, as compared to 69.5°, 66.6°, and 58° from the corresponding X-ray structures. However, the last X-ray value is based on the dppp structure of **4** as a surrogate for that of **3**.

Two mechanistic pathways were considered for the reductive elimination process: (1) phosphine ligand loss followed by reductive elimination from a three-coordinate intermediate and (2) reductive elimination from the four-coordinate complexes. The first process has a much greater total activation energy than the second and is inconsistent with the absence of a free phosphine influence on the reductive elimination rates. The second process is also consistent with the majority of studies on related complexes.[4,26−33] Direct reductive elimination from the four-coordinate complexes is therefore considered to be operative (Scheme 1).

Transition states (**1′-TS**, **2′-TS**, and **3′-TS**) were readily located using potential energy scans over the Pt-bonded carbon atom distance (C1--C7). Subsequent optimization proceeded smoothly for **1′-TS** and **3′-TS** but failed to converge for **2′-TS** due to low-energy (±0.06 kcal) PMe_3 group oscillations. Optimization with force constant calculation at each step did not correct the problem. Therefore, a minimum energy structure was selected as representative of **2′-TS**. A frequency calculation for this structure and for **1′-TS** and **3′-TS** showed a single imaginary frequency with the expected vibrational mode. Computed activation parameters are listed in Table 3, and although $\Delta H^{\ddagger}$ values are lower by a few kilocalories, the parameters match the experimental results very well including the larger gap in energy between **2** and **3** than between **1** and **2**. Selected metrical parameters for the optimized structures are given in Table 4, and a drawing of **3′-TS** is provided in Figure 4.

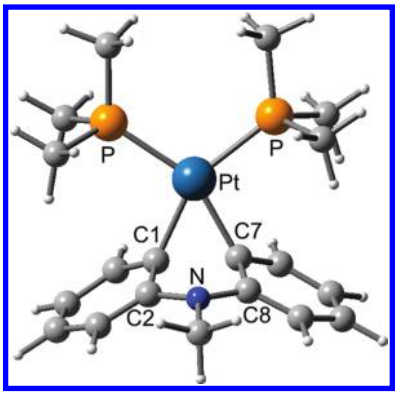

Figure 4. GaussView[34] drawing of **3′-TS**.

As would be expected, the transition-state structures all show a decrease in the C1−Pt−C7 angle, a lengthening of the Pt−C distance, and a reduction in the C1–C7 distance. Simultaneously, there is a reduction in the Pt−P distance and a widening of the P−Pt−P angle consistent with the incipient formation of the linear $Pt(PMe_3)_2$ fragment. These features are very similar to those of transition-state structures calculated for biphenyl reductive elimination from diaryl Pt and Pd complexes[27−29] and account for the much greater stability of **4** and **5** over **3**. The chelating ligands of **4** and **5** prevent widening of the L−Pt−L angle, thereby destabilizing the reductive elimination transition state.

The boat configuration with the Pt atom at the "bow" and X at the "stern" is still observed, but the Pt atom has moved up and back toward the "stern". This has moved the Pt atom into position for bonding with the aryl π-systems and begins to free the C sp^2 orbital for formation of the incipient C−C bond. In the eliminating organic component there is an increase in planarity, as shown by the decrease in the acute angle between the aryl rings and a decrease in the C2−X−C8 angle consistent with the beginning formation of the five-membered ring. There is also a decrease in the X−C2, C8 distance though it is

(25) Merwin, R. K.; Schnabel, R. C.; Koola, J. D.; Roddick, D. M. *Organometallics* **1992**, *11*, 2972–2978.
(26) Brune, H. A.; Falck, M.; Hemmer, R.; Alt, H. G. *Chem. Ber.* **1984**, *117*, 2803–14.
(27) Pérez-Rodríguez, M.; Braga, A. A. C.; Garcia-Melchor, M.; Pérez-Temprano, M. H.; Casares, J. A.; Ujaque, G.; de Lera, A. R.; Álvarez, R.; Maseras, F.; Espinet, P. *J. Am. Chem. Soc.* **2009**, *131*, 3650–3657.
(28) Yi-Luen, H.; Chia-Ming, W.; Fung, E. H. *Chem.−Eur. J.* **2008**, *14*, 4426–4434.
(29) Ananikov, V. P.; Musaev, D. G.; Morokuma, K. *Organometallics* **2005**, *24*, 715–723.
(30) Brown, J. M.; Cooley, N. A. *Chem. Rev.* **2002**, *88*, 1031–1046.
(31) Edelbach, B. L.; Lachicotte, R. J.; Jones, W. D. *J. Am. Chem. Soc.* **1998**, *120*, 2843–2853.
(32) Stang, P. J.; Kowalski, M. H.; Schiavelli, M. D.; Longford, D. *J. Am. Chem. Soc.* **1989**, *111*, 3347.
(33) Himmel, S. E.; Young, G. B. *Organometallics* **1988**, *7*, 2440–50.

very small in **1′-TS** (X = CH_2). For **2′-TS** (X = O) and **3′-TS** (X = NMe) the greater decrease is attributed to increased lone pair donation into the aromatic rings.

In comparing the three transition states there are trends in the metrical parameters indicating that the transition state occurs earlier in the reductive elimination process in the order **3′-TS** earlier than **2′-TS** earlier than **1′-TS**. This is seen in the order of the Pt−C1, C7 distances, **3′-TS** < **2′-TS** < **1′-TS**, the C1–C7 distances, **3′-TS** > **2′-TS** > **1′-TS**, and the P−Pt−P angles, **3′-TS** < **2′-TS** < **1′-TS**. Earlier stabilization is likely due to lone pair donation into the π-system with incipient aromatization on C1−C7 bond formation. Donation from the NMe group is stronger and the final product, *N*-methylcarbazole, is more aromatic than dibenzofuran, the final product with X = O. With X = CH_2, there is no possibility of aromaticity in the ring system. These arguments are consistent with the Hammond postulate, where greater stabilization of the product will shift the transition state toward the reactant.[35]

Discussion

Our initial interest in the six-membered platinacycles **1**−**3** was in the possibility of colloidal Pt catalysis of their reductive elimination reactions. We have shown previously that alkyne complex **6** in the presence of even traces of O_2 suffers oxidative deligation at 120 °C to produce colloidal Pt and that the colloidal Pt catalyzes reductive eliminations and alkyne cycloadditions of four- and five-membered platinacycles (eqs 4 and 5) and palladacycles.[13,14] The lack of any change in the reductive elimination kinetics of eq 3 for **1** in the presence of O_2 indicates that if colloidal Pt can participate in reductive elimination from **1**, the process is energetically too high to compete with direct reductive elimination. For the planar four- and five-membered metallacycles **7** and **8** the rate-limiting step in the colloidal Pt-catalyzed process appears to be transmetalation of the metallacycle to the colloid surface. Given the nonplanarity of **1**, the barrier to transmetalation may be higher than for the planar metallacycles. Unfortunately, little is known about factors associated with transmetalation to metal surfaces, a process that is also significant in OMCVD[36,37] and of potential application in the manipulation of carbon nanotubes.

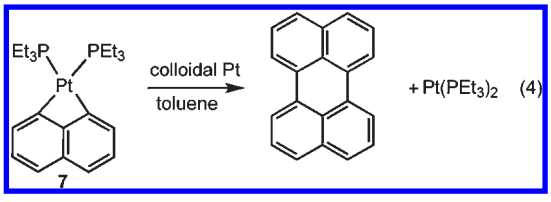

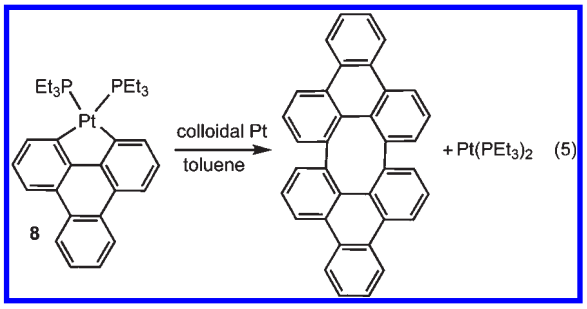

The relative ease of direct reductive elimination from platinacycles **1**−**3** as compared to **7** and **8** is associated primarily with the larger ring size. We know from oxidative addition studies of biphenylene to Pt(0) complexes that the energies for biphenylene reductive elimination from five-membered biphenyl platinacycle are unfavorable.[31,38] Direct elimination from **8** would require the formation of a strained four-membered biphenylene, even more strained than parent biphenylene. Direct elimination from **7** would form a three-membered ring that would be extremely unfavorable.

Reductive elimination from **1**−**3** should share features with reductive elimination from the diaryl complexes *cis*-$PtL_2(C_6H_4R)_2$. While the best comparison would be with 2-substituted *cis*-$PtL_2(C_6H_4\text{-}2\text{-}R)_2$, the complexes that have been most studied are 3- and 4-substituted *cis*-$PtL_2(C_6H_4\text{-}4\text{-}R)_2$. Strong similarities should still be observed and the behavior of *cis*-$PtL_2(C_6H_4\text{-}4\text{-}R)_2$ with R = CH_3, OMe, and NMe_2 would be expected to show parallels to **1**−**3**, where X = CH_2, O, NMe. A reductive elimination kinetic study of this series with L_2 = dppf (1,1′-bis(diphenylphosphino)ferrocene) was recently reported.[7] Activation parameters were not determined, but first-order rate constants at 95 °C are 15.5×10^{-5} s^{-1} (R = CH_3), 5.35×10^{-5} s^{-1} (R = OMe), and 32.3×10^{-5} s^{-1} (R = NMe_2). As with **1**−**3**, the fastest rate is observed for the nitrogen derivative, but the rates for the oxygen and carbon derivatives are inverted from that for **1**−**3**. For comparison, calculated rate constants for **1**−**3** at 95 °C are 0.466×10^{-5} s^{-1} (X = CH_2), 71.0×10^{-5} s^{-1} (X = O), and $2\,800\,000 \times 10^{-5}$ s^{-1} (X = NMe). Similar substituent effects are observed, but the changes are vastly greater with **1**−**3**. The rates for **1** and the diaryl complexes are similar, but the rate for **3** is millions of times greater than for the R = NMe_2 diaryl complex.

A larger substituent effect with a trend matching that of **1**−**3** is observed for the asymmetric diaryl complexes *cis*-Pt(dppf)(C_6H_4-4-R)(C_6H_4-4-CF_3), where the rate constants at 95 °C are 17.6×10^{-5} s^{-1} (R = CH_3), 23.3×10^{-5} s^{-1} (R = OMe), and 159×10^{-5} s^{-1} (R = NMe_2).[7] The effect is greater than with the symmetric diaryl complexes but is still orders of magnitude less than for **1**−**3**. We believe these larger effects are due to lone pair electron delocalization in the transition states. The very large effect observed in **3** and to a lesser extent in **2** is due to the beginning of aromatization of the ring system with the formation of the C−C bond. The N lone pair begins to delocalize over the entire ring system, strongly stabilizing the transition state. A similar, though less dramatic stabilization of the transition state occurs for the asymmetric diaryl *cis*-Pt(dppf)(C_6H_4-4-R)(C_6H_4-4-CF_3) when R = NMe_2, where the formation of the C−C bond allows electron density from the electron-rich C_6H_4-4-NMe_2 ring to delocalize into the relatively electron-poor C_6H_4-4-CF_3 ring. Alternatively, this can be viewed in terms of the Hammond postulate, where greater stabilization of the product by electron delocalization shifts the transition state toward the reactant.[35]

(34) *GaussView 3.0*; Gaussian, Inc., 2003.
(35) Hammond, G. S. *J. Am. Chem. Soc.* **1955**, *77*, 334–338.
(36) Zinn, A.; Niemer, B.; Kaesz, H. D. *Adv. Mater.* **1992**, *4*, 375–378.
(37) Mark, J.; Hampden-Smith, T. T. K. *Chem. Vap. Disposition* **1995**, *1*, 8–23.
(38) Perthuisot, C.; Edelbach, B. L.; Zubris, D. L.; Simhai, N.; Iverson, C. N.; Muller, C.; Satoh, T.; Jones, W. D. *J. Mol. Catal. A: Chem.* **2002**, *189*, 157–168. Simhai, N.; Iverson, C. N.; Edelbach, B. L.; Jones, W. D. *Organometallics* **2001**, *20*, 2759–2766.

Conclusion

Six-membered diaryl platinacycle complexes $Pt(C_6H_4X\text{-}C_6H_4)L_2$ (X = CH_2, O, or NMe and L = PEt_3, L_2 = 1,3-bis(phenylphosphino)propane (dppp) or 4,4′-bis-*tert*-butyl-2,2′-bipyridine ($^tBu_2bpy$)) are readily synthesized in >80% yield. Similar to related diaryl complexes $PtL_2(C_6H_4\text{-}R)_2$, direct reductive elimination from the L = PEt_3 derivatives **1**−**3** is observed with rates that depend on the ring substituent. However, the rates for the platinacycles **1**−**3** are dramatically more dependent on the bridging group X. The more than million-fold increase in the rate from **1** (X = CH_2) to **3** (X = NMe) is attributed to aromatic stabilization of the transition state for **3** by nitrogen lone pair donation. A much weaker effect is observed for **2** (X = O).

Experimental Section

All procedures were performed under a dinitrogen atmosphere in a Vacuum Atmospheres Corporation drybox unless otherwise stated. All solvents used were dried by standard techniques and degassed, then stored under dinitrogen over 4 Å molecular sieves or sodium metal. *N*-Methyldiphenylamine, 2,2′-dibromobenzophenone, *n*-butyllithium, diphenylacetylene, triethylphosphine (10 wt % in hexane), and diphenyl ether were obtained from commercial sources (Aldrich, Acros, or Strem) and used as received. *cis*-$PtCl_2(PEt_3)_2$,[39] Pt(dppp)Cl_2,[40] Pt(4,4′-bis-*tert*-butyl-2,2′-bipyridine)Cl_2,[41] 2,2′-dilithiodiphenyl-*N*-methylamine,[42] and 2,2′-dibromodiphenylmethane[43,44] were prepared by literature methods.

NMR spectra were recorded on Bruker AMX-250, -300, or -500 spectrometers at ambient probe temperature unless otherwise stated. Chemical shifts (δ) are given in ppm and coupling constants (J) in Hz. The ^1H shifts are relative to an internal TMS (0 ppm) standard (referenced to protio solvent signals), and the ^{13}C shifts are relative to internal solvent signal standard. The ^{31}P shifts are relative to an external 85% H_3PO_4 (0 ppm) standard, and the ^{195}Pt shifts are relative to an external K_2PtCl_4/D_2O (−1624 ppm) standard. Columbia Analytical Services, Inc. preformed the microanalyses.

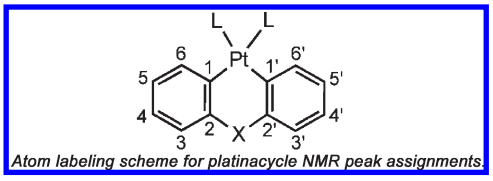

Atom labeling scheme for platinacycle NMR peak assignments.

Preparation of $Pt(C_6H_4CH_2C_6H_4)(PEt_3)_2$ (1). This is a modification of the reported procedure.[15] A colorless solution of 2,2′-dibromodiphenylmethane (28.4 mg, 0.0871 mmol) in 2 mL of THF was cooled to −30 °C in a refrigerator. The colorless solution was removed from the refrigerator, and *n*-BuLi (0.070 mL, 0.18 mmol, 2.5 M in hexanes) was added dropwise to the stirred colorless solution over a 10 min period. The resulting dark orange solution was stirred another 10 min and then replaced in the refrigerator for ca. 30 min. This orange solution was slowly added dropwise into a stirred suspension of *cis*-$Pt(PEt_3)_2Cl_2$ (46.4 mg, 0.0924 mmol) in 2 mL of THF, previously cooled to −30 °C in the refrigerator. The resulting bright orange mixture was stirred for 1 h and allowed to warm to room temperature. This solution was filtered through diatomaceous earth and the solvent removed under reduced pressure to give an orange oil. This oily product was washed twice with Et_2O and dried under reduced pressure to give **1** as a white solid. Yield: 16 mg (30.7%). ^{31}P NMR ($CDCl_3$, 101 MHz): 4.8 (s with satellites, J_{Pt-P} = 1833 Hz). ^{195}Pt NMR ($CDCl_3$, 64 MHz): −4574 (s with satellites, J_{P-Pt} = 1886 Hz).

Preparation of 2,2′-Dilithiodiphenyl Ether. This procedure is based on a reported *in situ* preparation.[42] A colorless solution of diphenyl ether (1073 mg, 6.304 mmol) in 5 mL of THF was cooled to −30 °C in a refrigerator. The solution was removed from the refrigerator, and while being stirred, ^{n}BuLi (5.30 mL, 13.3 mmol, 2.5 M in hexanes) was added dropwise into the stirred Ph_2O solution over a 10 min period. The resulting bright orange solution was stirred and allowed to warm to room temperature overnight. A white solid formed within the bright orange solution. The solution was decanted and the white solid was washed twice with cold hexane. The white solid product was dried *in vacuo*. Yield: 411.9 mg (35.8%). A few milligrams were treated with D_2O, and the mixture was extracted with $CDCl_3$. The ^1H NMR indicated the formation of 2,2′-dideuterodiphenyl ether: ^1H NMR ($CDCl_3$, 250 MHz): 7.31 (m, 4H, *m*-H), 7.08 (td, J_{H-H} = 7.4 and 1.2 Hz, 2H, *o*-H), 7.01 (dd, J_{H-H} = 8.4 and 1.2 Hz, 2H, *p*-H). The bright orange solution remaining after separation of the product was dried under reduced pressure, and the resulting orange residue was also treated with D_2O. The mixture was extracted with $CDCl_3$ for ^1H NMR, which indicated that the remaining material was mostly the product.

Synthesis of $Pt(C_6H_4OC_6H_4)(PEt_3)_2$ (2). A colorless solution of 2,2′-dilithiodiphenyl ether (152 mg, 0.835 mmol) in 2 mL of THF was cooled to −30 °C in a refrigerator. The cold solution was slowly added dropwise to a stirred suspension of $Pt(PEt_3)_2Cl_2$ (425 mg, 0.846 mmol) in 2 mL of THF, previously cooled to −30 °C. The resulting light yellow solution was stirred for 2 h and allowed to warm to room temperature. The yellow solution was filtered through diatomaceous earth and the solvent removed under reduced pressure to give a yellow oil. This was washed twice with MeOH and dried under reduced pressure to give **2** as a white solid. Yield: 425 mg (85.0%). Colorless single crystals for X-ray analysis were grown by slow vapor diffusion of MeOH into a C_6H_6 solution at room temperature. Anal. Calcd (%) for $C_{24}H_{38}OP_2Pt$: C, 48.08; H, 6.39. Found: C, 47.82; H, 6.06.

^1H NMR (C_6D_6, 300 MHz): 7.69 (td with satellites, J_{H-H} = 7.2 and 1.8 Hz, J_{Pt-H} = 60.5 Hz, 2H, $H_{2,2'}$), 7.53 (dd, J_{H-H} = 7.8 and 1.5 Hz, 2H, $H_{5,5'}$), 7.06 (td, J_{H-H} = 7.2 and 1.5 Hz, 2H, $H_{4,4'}$), 6.99 (t, J_{H-H} = 6.9 Hz, 2H, $H_{3,3'}$) 1.37 (m, 6H, CH_2), 0.76 (m, 9H, CH_3). ^{13}C NMR (C_6D_6, 125 MHz): 160.9, 138.9, 128.4, 124.2, 122.4, 117.8, 17.1−16.6 (m), 8.2 (s with satellites, J_{Pt-C} = 19.1 Hz). ^{13}C NMR ($CDCl_3$, 75 MHz): 159.8 (s with satellites, J_{Pt-C} = 26.4 Hz, $C_{2,2'}$), 145.3 (dd with satellites, J_{P-C} = 105.7 and 10.6 Hz, J_{Pt-C} = 769.7 Hz, $C_{1,1'}$), 138.4 (t, J_{P-C} = 7.5 Hz, $C_{5,5'}$), 123.5 (s, $C_{4,4'}$), 122.2 (t with satellites, J_{Pt-C} = 58.1 Hz, J_{P-C} = 3.0 Hz, $C_{6,6'}$), 116.8 (s with satellites, J_{Pt-C} = 18.8, $C_{3,3'}$), 17.0−16.3 (m, PEt_3-CH_2), 8.2 (s with satellites, J_{Pt-C} = 18.8 Hz, PEt_3-CH_3). ^{31}P NMR ($CDCl_3$, 101 MHz): 5.0 (s with satellites, J_{Pt-P} = 2014 Hz). ^{31}P NMR (C_6D_6, 101 MHz): 5.3 (s with satellites, J_{Pt-P} = 2002 Hz). ^{195}Pt NMR ($CDCl_3$, 64 MHz): −3112 (s with satellites, J_{P-Pt} = 2015 Hz).

Synthesis of $Pt(C_6H_4NMeC_6H_4)(PEt_3)_2$ (3). A suspension of $Pt(PEt_3)_2Cl_2$ (45.2 mg, 0.0900 mmol) in 2 mL of THF was cooled to −78 °C in an acetone/dry ice bath. Then, a light yellow solution of 2,2′-dilithiodiphenyl-*N*-methylamine (35.8 mg, 0.0837 mmol)

(39) Parshall, G. W. *Inorg. Synth.* **1970**, *12*, 26–33.
(40) Appleton, T. G.; Bennett, M. A.; Tomkins, I. B. *J. Chem. Soc., Dalton Trans.* **1976**, 439–46.
(41) Rendina, L. M.; Vittal, J. J.; Puddephatt, R. J. *Organometallics* **1995**, *14*, 1030–1038.
(42) Braddock-Wilking, J.; Corey, J. Y.; French, L. M.; Choi, E.; Speedie, V. J.; Rutherford, M. F.; Yao, S.; Xu, H.; Rath, N. P. *Organometallics* **2006**, *25*, 3974–3988.
(43) Bickelhaupt, F.; Jongsma, C.; De Koe, P.; Lourens, R.; Mast, N. R.; Van Mourik, G. L.; Vermeer, H.; Weustink, R. J. M. *Tetrahedron* **1976**, *32*, 1921–1930.
(44) Lee, W. Y.; Park, C. H.; Kim, Y. D. *J. Org. Chem.* **1992**, *57*, 4074–4079.

in 2 mL of THF, previously cooled to −78 °C, was quickly added into the stirred suspension. The resulting yellow mixture was slowly warmed to −40 °C. Due to the instability of **3** above −30 °C, a sample could not be isolated and characterization is limited to *in situ* NMR spectroscopy and reactivity.

^{13}C NMR (THF, 75 MHz, −40 °C): 151.7, 144.2, 137.3, 121.7, 118.7, 111.6, 35.3, 16.0−15.6 (m), 7.6. ^{31}P NMR (THF, 121 MHz, −30 °C): 7.3 (s with satellites, J_{Pt-P} = 1979 Hz). ^{31}P NMR (toluene, 101 MHz, −20 °C): 5.7 (s with satellites, J_{Pt-P} = 1998 Hz). ^{195}Pt NMR (THF, 64 MHz, −40 °C): −4700 (s with satellites, J_{P-Pt} = 2007 Hz).

Synthesis of Pt($C_6H_4NMeC_6H_4$)(1,3-bis(diphenylphosphino) propane) (4). A light yellow solution of 2,2′-dilithiodiphenyl-*N*-methylamine (21.1 mg, 0.0494 mmol) in 2 mL of THF was cooled to −30 °C in a refrigerator. The solution was slowly added dropwise into a stirred suspension of Pt(dppp)Cl_2 (38.8 mg, 0.0572 mmol) in 2 mL of THF, previously cooled to −30 °C in a refrigerator. The resulting light yellow solution was stirred for 30 min and allowed to warm to room temperature. The yellow solution was filtered through diatomaceous earth and the solvent removed under reduced pressure to give a bright yellow precipitate. The precipitate was washed twice with ether and dried under reduced pressure to give **4** as a bright yellow solid. Yield: 32.7 mg (84.1%). Bright yellow single crystals for X-ray analysis were grown by slow vapor diffusion of Et_2O into a C_6H_6 solution at room temperature. Anal. Calcd (%) for $C_{40}H_{37}NP_2Pt$: C, 60.91; H, 4.73; N, 1.78. Found: C, 60.50; H, 4.46; N, 2.17.

^{1}H NMR ($CDCl_3$, 300 MHz): 7.96 (b, 4H, *p*-Ph), 7.40 (b, 8H, *m*-Ph), 7.09 (b, 8H, *o*-Ph), 7.01 (d, J_{H-H} = 7.2 Hz, 2H, $H_{5,5'}$), 6.77 (d with satellites, J_{H-H} = 8.1 Hz, J_{Pt-H} = 74.1 Hz, 2H, $H_{2,2'}$), 6.55 (t, J_{H-H} = 7.8 Hz, 2H, $H_{3,3'}$), 5.89 (t, J_{H-H} = 7.2 Hz, 2H, $H_{4,4'}$), 3.37 (s, 3H, NMe), 2.46 (b, 2H, propyl), 2.19 (b, 4H, propyl). ^{13}C NMR (C_6D_6, 125 MHz): 149.7, 141.9, 135.3, 132.6, 130.2, 127.3, 123.3, 120.6, 112.8, 67.8, 45.9, 37.3, 25.8, 20.1. ^{31}P NMR ($CDCl_3$, 101 MHz): 3.6 (s with satellites, J_{Pt-P} = 1902 Hz). ^{31}P NMR (C_6D_6, 101 MHz): 4.1 (s with satellites, J_{Pt-P} = 1884 Hz). ^{195}Pt NMR ($CDCl_3$, 64 MHz): −3079 (s with satellites, J_{P-Pt} = 1905 Hz).

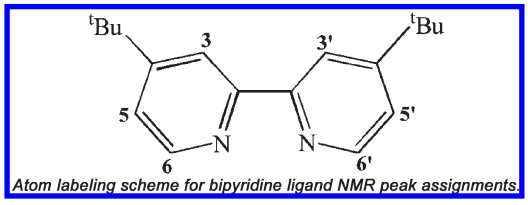

Atom labeling scheme for bipyridine ligand NMR peak assignments.

Synthesis of Pt($C_6H_4NMeC_6H_4$)(4,4′-bis-*tert*-butyl-2,2′-bipyridine) (5). A light yellow solution of 2,2′-dilithiodiphenyl-*N*-methylamine (20.6 mg, 0.0482 mmol) in 2 mL of THF was cooled to −30 °C in a refrigerator. The solution was slowly added dropwise into a stirred suspension of Pt(^{t}Bu$_2$bpy)Cl_2 (32.0 mg, 0.0599 mmol) in 2 mL of THF, previously cooled to −30 °C in the refrigerator. The resulting dark purple solution was stirred for 30 min and allowed to warm to room temperature. The solution was filtered through diatomaceous earth and the solvent removed under reduced pressure. The dark residue was washed twice with MeOH and dried under reduced pressure to give **5** as a dark purple solid. Yield: 26.4 mg (84.9%). Bright red crystals for the X-ray analysis were grown by slow vapor diffusion of EtOH into a C_6H_6 solution at room temperature. Anal. Calcd (%) for $C_{31}H_{35}N_3Pt$: C, 57.75; H, 5.47; N, 6.52. Found: C, 57.86; H, 5.71; N, 6.05.

^{1}H NMR ($CDCl_3$, 500 MHz): 9.07 (d, J_{H-H} = 6.0 Hz, 2H, bpy-$H_{6,6'}$), 7.98 (d, J_{H-H} = 1.5 Hz, 2H, bpy-$H_{3,3'}$), 7.48 (d with satellites, J_{H-H} = 7.0 Hz, $J_{Pt-H} \approx$ 61.3 Hz, 2H, $H_{2,2'}$), 7.47 (dd, J_{H-H} = 6.0 and 2.0 Hz, 2H, bpy-$H_{5,5'}$), 7.00 (t, J = 8.0 Hz, 2H, $H_{3,3'}$), 6.85 (d, J = 8.0 Hz, 2H, $H_{5,5'}$), 6.79 (t, J = 7.0 Hz, 2H, $H_{4,4'}$), 3.31 (s, 3H, NMe), 1.42 (s, 18H, ^{t}Bu). ^{13}C NMR ($CDCl_3$, 125 MHz): 162.0, 156.1, 152.2, 150.0, 137.5, 128.3, 123.3, 123.0, 120.1, 118.4, 111.5, 36.6, 35.6, 30.3. ^{195}Pt NMR ($CDCl_3$, 64 MHz): −3646.

Thermolysis of Pt($C_6H_4CH_2C_6H_4$)(PEt_3)$_2$ (1) and Pt(C_6H_4-OC_6H_4)(PEt_3)$_2$ (2). Solutions for kinetic studies of both **1** and **2** were prepared similarly by dissolving 5.0 ± 0.3 mg of the platinacycle (0.0084 mmol of **1** or 0.0083 mmol for **2**) and 14.0 ± 0.5 mg of PhCCPh (0.079 mmol) into 0.300 ± 0.001 mL of toluene. The colorless solutions containing 0.028 M platinacycle were placed into 5 mm NMR tubes, topped with a plastic cap, and further sealed with wax film to prevent exposure to air during the experiment. A ^{31}P NMR spectrum was taken at room temperature to validate purity and the relative concentrations of the sample. The sample was then inserted into the preheated probe of the Bruker AMX-250 spectrometer at the appropriate temperature, and ^{31}P NMR spectra were recorded every 15 min until at least 90% of the platinacycle had decomposed. The final solutions were homogeneous and yellow. Experiments without PhCCPh addition showed that the added PhCCPh had no effect on the reaction rates.

Decomposition of Pt($C_6H_4NMeC_6H_4$)(PEt_3)$_2$ (3). *cis*-Pt-(PEt_3)$_2Cl_2$ (11.0 ± 0.3 mg, 0.022 mmol) suspended in 0.30 ± 0.001 mL of toluene was placed into a 5 mm screw-capped NMR tube. The NMR tube was capped with a septum cap and further sealed with wax film. A light yellow solution of 2,2′-dilithiodiphenyl-*N*-methylamine (10.0 ± 0.3 mg, 0.023 mmol) dissolved in 0.20 ± 0.001 mL of toluene was loaded into a 1.0 mL syringe. The NMR tube was cooled to −78 °C in an acetone/dry ice bath, and then the Li solution was slowly added, being careful not to increase the resulting solution's temperature. (Assumed concentration of **3**: 0.044 M at 100% yield.) The NMR tube was again sealed with wax film to prevent exposure to air during the experiment. The sample was then inserted into the precooled probe of a Bruker AMX-250 spectrometer at the appropriate temperature, and ^{31}P NMR spectra were recorded every 15 min until at least 90% of the platinacycle had decomposed, resulting in a yellow solution.

Thermolysis of 1 with Added O_2 and Air. (a) O_2: A 5 mm screw-capped NMR tube was charged with 5.0 ± 0.3 mg of **1** (0.0084 mmol) and 14.0 ± 0.5 mg of PhCCPh (0.079 mmol) dissolved into 0.3 ± 0.01 mL of toluene. The NMR tube was capped with a septum cap and sealed with wax film. Molecular oxygen (5.0 ± 0.1 mL, 0.22 mmol) was injected into the NMR tube using a syringe. The NMR tube was again sealed with more wax film. (b) Air: A solution of 5.0 ± 0.3 mg of **1** (0.0084 mmol) dissolved into 0.3 ± 0.01 mL of toluene was exposed to air for several minutes. The solution was then placed into a 5 mm NMR tube and capped. The samples were inserted into the preheated probe of the Bruker AMX-250 spectrometer at 120 or 130 °C, and ^{31}P NMR spectra were recorded every 15 min until at least 90% of the platinacycle had decomposed.

Thermolysis of 2 with Added H_2O and PEt_3. (a) H_2O: A 5 mm NMR tube was charged with 5.0 ± 0.3 mg of **2** (0.0083 mmol) dissolved in 0.300 ± 0.01 mL of toluene. One drop of DI H_2O was added. (b) PEt_3: A 5 mm NMR tube was charged with 5.0 ± 0.3 mg of **2** (0.0083 mmol) dissolved in 0.22 ± 0.01 mL of toluene. PEt_3 (10 wt % in hexane, 0.080 ± 0.001 mL, 0.045 mmol) was added. The samples containing 0.028 M **2** were capped and sealed with wax film. The samples were then inserted into the preheated probe of the Bruker AMX-250 spectrometer at 90 °C, and ^{31}P NMR spectra were taken every 15 min until at least 90% of the platinacycle had decomposed.

Computational Details. Gaussian 03[45] with the B3LYP[46] functional was used for all calculations (gas phase). The LANL2DZ[47−50] basis set was employed for Pt and P with added

(45) *Gaussian 03, Revision B.04*; Gaussian, Inc., **2003** (see SI for full reference).
(46) Becke, A. D. *J. Chem. Phys.* **1993**, *98*, 5648.
(47) Dunning, T. H.; Hay, J. P. *Modern Theoretical Chemistry*; Plenum: New York, 1976; Vol. *3*.
(48) Hay, P. T.; Wadt, W. R. *J. Chem. Phys.* **1985**, *82*, 270.
(49) Wadt, W. R.; Hay, P. T. *J. Chem. Phys.* **1985**, *82*, 284.
(50) Hay, P. T.; Wadt, W. R. *J. Chem. Phys.* **1985**, *82*, 299.

d-diffuse functions for Pt ($\alpha = 0.05$) and d-diffuse ($\alpha = 0.364$) and p-polarization ($\alpha = 0.0298$) functions for P.[51] The 6-31G(d, p) basis set was used for all other atoms. All geometries were optimized (no symmetry constraints) and energies zero-point-corrected. Free energies, enthalpies, and entropies were calculated at 298.15 K and 1 atm. Analytical frequency calculation gave no imaginary frequencies for the reactants and one imaginary frequency for the transition states. Examination of the corresponding vibrational modes for the imaginary frequencies with GaussView[34] showed these to be consistent with the products and reactants. In cases where the nature of the vibrational mode was unclear an IRC calculation or geometry optimization of the structure after slight displacement along the vibrational mode direction demonstrated connection with the reactant and product.

(51) Check, C. E.; Faust, T. O.; Bailey, J. M.; Wright, B. J.; Gilbert, T. M.; Sunderlin, L. S. *J. Phys. Chem. A* **2001**, *105*, 8111.

Acknowledgment. We thank NSF for early, initial, partial support of this work (CHE-0406353) and the University of Missouri for a Gus T. Ridgel Fellowship (R.R.). A grant from the National Science Foundation (9221835) provided a portion of the funds for the purchase of the NMR equipment. We also thank Dr. C. Barnes for X-ray support, Dr. W. Wei for NMR support, and Dr. C. Deakyne for DFT support.

Supporting Information Available: CIF files for the crystal structures, kinetic data, and DFT results. This material is available free of charge via the Internet at http://pubs.acs.org.